STUDY OF THE FILM FORMATION PROCESS IN LIQUID–LIQUID EXTRACTION FLOW INJECTION ANALYSIS

Vlastimil KUBÁŇ*

Department of Analytical Chemistry,
Royal Institute of Technology, S-10044 Stockholm, Sweden

Received August 31st, 1990
Accepted November 6th, 1990

The behaviour of a thin film of an organic solvent on the walls of the extraction coil in a continuous liquid–liquid extraction flow system was studied using a computer-controlled fast-recording "on-tube" photometric detection system (approx. 3 ms time resolution). A single-loop injector was employed to introduce precise, reproducible volumes ($S_r < 2\%$) of one phase into the continuous stream of the other as a segmented volume standard. The film thickness d_f, ranging from 1 to 20 μm for a 0·7 mm teflon tube, was calculated from the segment lengthening at different chloroform flow rates and was found to obey a polynomial dependence on the linear flow rate, $d_f = f(u^\alpha)$, where $\alpha < 1$.

Liquid–liquid extraction in flow injection analysis (FIA) (refs[1–4]) is very efficient even under conditions where the organic and especially the aqueous phase segments are relatively large. The extraction efficiency in the extraction coil is usually high and the extraction is often virtually complete in a few seconds. These parameters are a result of the mechanism of FIA liquid–liquid extraction in narrow capillary tubes, which is mainly dependent on the formation of a very thin film of one solvent on the inner capillary wall[5–7], surrounding the segments of the other phase.

Two basic mass transport mechanisms can be operative – transport through the vertical interfaces (menisci) between the two phases (axial extraction) and transport through the horizontal interfaces (the wetting film) on the tubing wall (radial extraction). The ratio of the interfacial area to the volume as well as other factors determine the predominating mechanism[5–10]. The magnitude of the contact area is determined mainly by the segment length in the extraction coil, so that the segmentation pattern must be controllable and constant during the entire analytical procedure.

The existence of a bridging film between adjacent segments of one of the phases stabilizes the entire segmented stream[11,12]. On the other hand, solute transfer can occur from one segment to the nighbouring segment of the same phase, as a result of mass transfer "backwards" from one organic segment to the subsequent organic

* Permanent address: Department of Analytical Chemistry, Masaryk University, 611 37, Brno, Czechoslovakia.

segments via the wetting film. The film thus plays an important role in peak broadening, i.e. in the dispersion and dilution of the sample. The thicker the film, the greater is the peak broadening.

These processes have been observed in earlier work and have been the subject of very detailed study, including peak height and peak area depression[13,14], sample dispersion and peak broadening[7,10,15] and the kinetics of the extraction process[11,12]. The extent of very good work carried out on the various parametric effects emphasizes the increasing need for a detailed fundamental study of the wetting film behaviour.

Our studies of the segmentation process in liquid–liquid extraction flow injection analysis revealed a marked increase in the segment length of the aqueous phase with increasing total flow rate[16]. In this work, a rotary loop injector was used to inject very precisely defined volumes of one immiscible phase into a continuously flowing stream of the other phase. The segments produced by the injections were employed to determine the wetting film thickness by measuring the lengthening of the water segments in a continuous stream of an organic solvent.

THEORETICAL

When a very precisely defined volume of one immiscible solvent is introduced into a continuously flowing stream of another solvent, the original shape of the solvent plug inside the loop injector becomes a spherical, ellipsoidal or deformed tubular segment inside the reaction/extraction tubing. The resulting segment shape depends primarily on the ratio between the segment volume and the inner radius of the tube, the total flow rate, the interfacial tension of the solvents, the surface tension of the solvents and the tubing material, as well as other factors.

A solvent displaying greater affinity for the material of the extraction capillary coil will cover its walls with a thin film with a relatively stationary nature; this will depend on the tubing material. The organic solvent film in a fluoropolymer tubing will surround the deformed spherical, ellipsoidal or tubular aqueous segments, while the segments of the organic phase in glass or metal tubing will be surrounded by an aqueous film.

The driving force for film formation is minimization of the interfacial energy at the solid/liquid interface, which is determined by the relative magnitudes of the surface tension of the inner tubing wall surface in contact with the liquids (wetting ability) and the interfacial tension of the liquids. Other factors influencing the formation of the wetting film include the hydrodynamic forces connected with the mass transport, resulting from the velocity distribution of the laminar flow across the tube profile, as the segment of the non-wetting solvent forms a compressible bolus flowing through the stream of the other solvent.

Additional factors affecting the segment shape include the mean value of the film

thickness (or the geometrical parameters of the "ring-like" orifice between the segment and the tubing walls) of one liquid behind a single plug of the other liquid that is moving through a capillary, where one phase preferentially wets the capillary surface in liquid systems containing two phases, which evidently depends on the linear velocity of the flowing stream, u, or its total flow rate, $Q_t = Q_a + Q_o$.

There is no exact theory of film formation in FIA liquid–liquid extraction systems. However, a number of equations have been derived for film formation in gas/liquid systems[17,18] and have been applied to liquid/liquid systems[7]. These equations have the form

$$d_f = kr_o(u\eta/\gamma_{o/a})^\alpha , \qquad (1)$$

where α and k are constants which usually equal[17,18] 1/2 and 2/3, respectively.

The film formed by one phase on the tubing walls as a result of a linear velocity distribution across the tubing cross-section and the wetting properties of the solvent affect the segment geometry[7,8]. Assuming a constant volume V_s of the segments of one immiscible phase (in this case, aqueous) in a continuous stream of the other phase permits prediction of the lengthening of the aqueous phase segment as a result of film formation on the tubing walls or of changes in the nearly cylindrical segment shape at zero flow rate to an ellipsoidal or deformed cylindrical shape, where the ends of the segments display a more or less characteristic convex (conceve) shape at higher flow rates[7,8].

The segment length L_s can be expressed as a function of the segment volume V_s and the outer radius of the cylindrical segment r_s, which depends on the inner radius of the tubing r_0 and the film thickness $d_f (r_s = r_o - d_f)$:

$$L_s = V_s/\pi r_s^2 = V_s/\pi(r_o - d_f)^2 . \qquad (2)$$

The segment length L_s is inversely proportional to the square of the outer segment radius r_s. With increasing film thickness d_f, the L_s value will increase as a result of the decreasing outer radius of the segment at higher flow rates or linear velocities. The relative segment lengthening decreases with increasing tube inner radius.

Assuming that the $(\eta/\gamma_{o/a})^\alpha$ term is constant during the experiments and substitution of the film thickness d_f from Eq. (*1*) into Eq. (*2*) permits expression of the segment length as a function of the linear velocity u:

$$L_s = V_s/\pi(r_o - k_u r_o u^\alpha)^2 = L_o/(1 - k'_u u^\alpha)^2 \qquad (3)$$

or as a function of the total flow rate $Q_t = Q_a + Q_o$:

$$L_s = V_s/\pi(r_o - k_q r_o Q_t^\alpha)^2 = L_o/(1 - k'_q Q_t^\alpha)^2 . \qquad (4)$$

Using different values for α and constants k_u, k'_u, k_q and k'_q ($\alpha = 0{\cdot}1-2$, $k = k' = 0{\cdot}1-1$) permits theoretical modelling of the effect of the linear velocity u or the total flow rate Q_t on the segment length L_s or its relative lengthening $(L_s - L_o)/L_o$. The resulting curves are always nonlinear with a shape that depends on both constants. The intercept on the L_s or $(L_s - L_o)/L_o$ axis corresponds to the original segment length L_o at zero linear velocity or total flow rate ($u \to 0$, $Q_t \to 0$) or is equal to zero. The segment length L_o can also be calculated from the originally injected volume V_s of the appropriate immiscible solvent as $L_o = V_s/\pi r_o^2$.

EXPERIMENTAL

Apparatus

The carrier phase stream was formed using a liquid chromatographic pump (Consametric III metering pump, LDC/Milton Roy, Riviera Beach, U.S.A.) with a flow rate of $Q_t < 10$ ml min^{-1}. The pump was equipped with a pulse damper and an Altech pressure indicator (Applied Science, U.S.A.). A restrictor column (50 × 4 mm, Hibar LiChroCART HPLC cartridge packed with LiChrosorb Si 60) mounted in a Hibar LiChroCART manu-fix 50-4 cartridge holder (E. Merck, Darmstadt, F.R.G.) ensures sufficient back pressure for proper action of the pump and the damper (see Fig. 1). The organic phase flow was developed in a displacement bottle with a volume of $V = 250$ ml by pumping the aqueous phase into it.

A single loop injector (6-port stopcock, Model 5020, Rheodyne, U.S.A.) with 100, 50 and 15 mm of 0·7 mm i.d. loop capillary was used for the injection of very precisely defined volumes of the aqueous or organic phase into a continuously flowing stream of the other phase, forming a standard segment length suitable for segment length and shape measurements. The motor-driven injection valve was mounted on a FIA 05 unit (Bifok A.B., Sweden). Alternatively, the given volume of one solvent was injected manually into a continuous stream of the other solvent under varying experimental conditions. A Gilson eight-channel peristaltic pump Minipuls 2 (Gilson Instruments, Villiers le Bel, France) was used to fill the injector loop.

The resulting segmented flow passes through the FEP or teflon extraction tube, in which the segment length equilibrates. Transparent FEP thin-wall tubing (Habia, Sweden) with 0·7 mm i.d. (0·15 mm wall thickness) and 0·7 mm i.d. teflon tubing (Tecator, Sweden) were tested. The tubing length was varied from 5 to 250 cm by changing the distance between the injection device and the detector flow dell, L_{EC}. Any effect from variation in the inner diameter of the FEP measuring

FIG. 1

Liquid–liquid extraction FIA manifold. P1 peristaltic pump, P2 HPLC pump with restrictor column and pressure indicator, B displacement bottle, L loop injector, coaxial segment or magnetic valve, E equilibration coil (teflon), M measuring transparent FEP tube, D on-tube photometric detector, C personal computer, R restriction coil, W waste, a aqueous phase, o organic phase

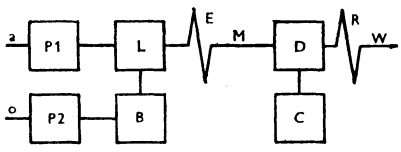

tube was eliminated by reversing the carrier stream flow direction for a given measuring point position (5/85, 10/80, 15/75 cm, etc. for a 90 cm total FEP tube length). A restriction coil (0·7 mm i.d., 2 m long teflon tube) was positioned beyond the detector flow cell to establish an appropriate back over-pressure.

The segment length was measured by a detector reading signal values across the tube (LKB. 2151 Variable Wavelength Monitor, LKB Bromme, Sweden), equipped with a special flow cell holder to allow the use of FEP transparent tubing. An analytical signal was produced by a variation in the refractive index and by changes in the absorptivity as segments of the two solvents passed through the detector. The analog detector signal from the logarithmic converter was fed to a Compaq Deskpro 286, Model 2 personal computer (Compaq Computer Corp., Houston, U.S.A.) via a PCI-20019M-1 high-speed data aquisition module, PCI-20010Z-1 analog termination panel and PCI-20012A-1 cable using PCI-20046S-6 series software driver language support subroutine libraries with a Basic language interface (Burr–Brown Corp., Tuscon, U.S.A.).

Procedure

Computer programs written in Basic were used for communication between the computer and the detector and for data treatment. After zero signal adjustment (for the aqueous, organic or segmented stream) and baseline noise determination, the signal level was sampled every 3, 6, 21 or 30 ms, depending on the segment length, to obtain a sufficient number of readings per segment ($n > 15$, $n > 50-200$ in most cases). An integration time of 9 or 21 ms was used to increase the precision of the measurement at the slower reading frequency. The measured values were either stored in the computer memory for post-run mathematical treatment or the data was treated immediately during the experiment.

The beginning of the segment was identified as the point at which the mean signal values of 7 (3) successive readings exceeded the $S_0 \pm 10\,s_0$ value. All "segments" with a duration of less than 30 ms were considered to be noise or "air bubble" signals and automatically excluded. The segment length, mean signal height, signal area and ratio of the signal area to duration were calculated for each segment. The mean values for all the segment parameters were then calculated for a full set of segments in a single run ($n = 20-100$ values), along with their statistical parameters. The mean of several runs (usually from 3 to 5) was used as the final length value. Graphic "on-screen" presentation of the stored data was used where required.

Chemicals

Water-saturated chloroform (E. Merck, F.R.G., analytical grade) was used. Aqueous 10 μM solutions of bromocresol green or neutral red were sometimes employed as coloring agents during segment length measurements. Distilled water and all the solutions were degassed in a Branson 2200 ultrasonic bath (Branson, U.S.A.).

RESULTS AND DISCUSSION

A plot of the analytical signal vs time for the organic phase segments in a continuous flowing stream of the aqueous phase of for the aqueous segments in a continuous stream of the organic phase at very low flow rates and low flow-rate ratios exhibits a characteristic, almost rectangular shape, which becomes deformed at higher flow rates (see Fig. 2).

The slopes of the central parts of the curves are close to zero for very long segments of either phase or for very low flow rates. They are mostly positive for shorter organic phase segments or higher flow rates, which also tend to shift the position of the plateau towards slightly higher values (<10%), especially at very high flow rates and high segment alteration frequencies. Film formation leads to an increase in both the baseline noise and the baseline signal. A more or less clear deformation of the horizontal parts of the curves was evident and can be attributed to film formation or destruction and also to fluctuation of the film thickness with time.

At high organic phase flow rates, Q_o, the aqueous segments have a rectangular wave shape with spikes of varying amplitude at the ends of the segment plateau (as described in the literature[7,8,19], but less marked) as a result of the sharper concave ends of the segments. The abrupt changes in the optical parameters of the surfaces of the menisci sometimes lead to the formation of negative peaks on the baseline at the beginnings or ends of the aqueous segments (see Fig. 2).

The typical shapes of the organic segments in the aqueous phase flowing stream (or of the aqueous segments in the organic phase stream) observed at different flow rates at a distance of 15 and 75 cm downstream from the injection point correspond to the lengthening of the ascending and descending parts of the curves for both segments. More convex or concave forms of the ascending and descending parts of the curve at higher flow rates are a result of the deformation of the strictly cylindrical shape of the segments in the injection loop to a more or less distorted cylindrical or semi-ellipsoidal shape inside the extraction coil. The characteristic paraboloid form of the leading and trailing ends of the segments is a result of film formation at the ends of the segments and of deformation of the segments as a result of hydrodynamic forces.

The length of the aqueous segments increases sharply with increasing flow rate of the organic phase. This effect is stronger for the 15 mm sample loop (<12%) than for the 50 mm and 100 mm loop capillaries (<9% and <7%, resp.) over the whole range of Q_o from 0·2 to 2 or 4 ml min^{-1}. The relative changes in segment

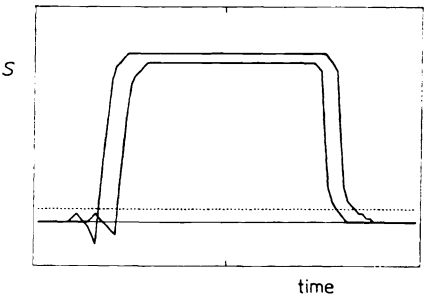

FIG. 2

Analytical signal (S) shape of the aqueous phase segments L_s = 50 mm at two different organic phase flow rates Q_o = 0·5 (lower curve) and 4 (upper curve) ml min^{-1}. The dashed line indicates the 10 s_o value

length obey a polynomial dependence on the flow rate with a slight plateau at higher flow rates above Q_o or Q_a of 3 ml min^{-1} (see Fig. 3).

The ratio of the analytical signal area to the signal duration increases for the aqueous segments by about 10% in the flow rate range Q_o from 0·15 to 2 ml min^{-1} and then remains practically constant at higher flow rates. The observed increase is greater for the shorter distance between the injection and detection points (L_{EC} = = 15 cm) than for the longer distance (L_{EC} = 75 cm).

The segmentation repeatability is impaired by increasing the length L_{EC} of the extraction capillary up to 250 cm and the total flow rate to 8 ml min^{-1} (see Fig. 4), with a minimum at the lower flow rates between 0·5 and 4 ml min^{-1}. The segmentation pattern is very regular (s_r < 10%) over a wide range of Q_a from 0·2 to 6 ml min^{-1}, Q_o from 0·2 to 5 ml min^{-1} and L_{EC} from 20 to 250 cm. Better segmentation repeatability (s_r < 2%) can be achieved by injecting the aqueous phase into the flowing organic phase than by the opposite procedure (s_r < 5%); in the former case, a stable film of organic phase is present on the tubing walls prior to the injection. The lower wetting of the teflon tubing by water is also important, especially for the rinsing process. The segmentation repeatability is better for 100 and 50 mm than for the 15 mm loop capillary length, but is satisfactory in all cases. Thus, the loop injector can be used for introducing precise sample volumes in immiscible fluid carrier continuous flow analysis (IFCCFA)[11,20].

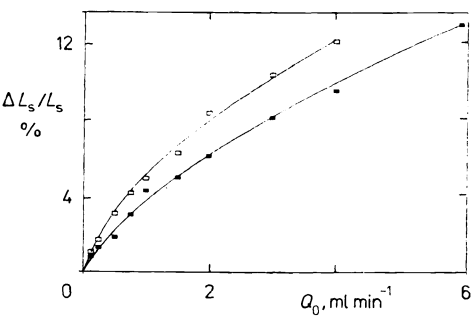

FIG. 3

Relative lengthening of the aqueous phase segment ($\Delta L_s/L_s$) in % as a function on the organic phase (chloroform) flow rate (Q_o in ml min^{-1}) for the loop injector (15 mm loop capillary) at distances of 15 and 75 cm from the injection point (open and full squares, respectively)

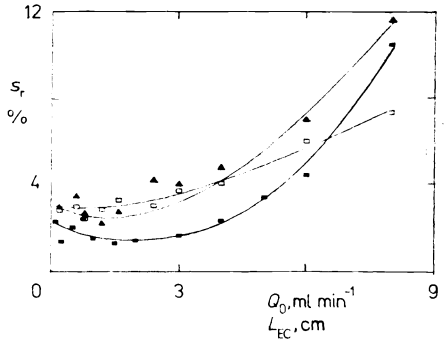

FIG. 4

Repeatability of the aqueous phase segment length (s_r in %) produced by the loop injector (50 mm loop, full squares) as a function of the flow rate (Q_o on ml min^{-1}) of the organic phase and the distance between the injection and measurement points (tube length L_{EC} in cm multiplied by 25) for 15 (triangles) and 50 (open squares) mm loop capillaries at Q_o = 4 ml min^{-1}

The low back pressure of the liquid chromatographic pump at low flow rates (under 0·1 ml min^{1}) results in a less repeatable segmentation pattern. Small droplets of the organic or aqueous phase are then formed at the leading or trailing ends of the segments as a result of incomplete rinsing of the sample loop at the low flow rates. The same phenomenon was also observed at very high flow rates ($Q_a > 8$ ml min^{-1}), probably as a result of destruction of the very narrow cylindrical segments or destruction of the very thick film of organic solvent on the teflon tubing walls formed at high flow rates when the interfacial forces are lower than the "Poiseuille" forces[16].

The length of the aqueous segments is always increased by the formation of a regular of the organic phase on the teflon or FEP tubing walls and as a result of the convex shape of both ends of the segments. Shorter segments are more strongly affected by film formation and the film is completely destroyed when very long aqueous segments alternate with relatively very short organic segments. The analytical signal measured on the aqueous segments decreases with decreasing alternation frequency of the aqueous segments or when a single segment of organic phase is introduced into a continuous stream of water. These results are in agreement with the observations of Dasgupta[11].

The film thickness depends on the flow rate, the flow rate ratio, the alternation frequency and the segment length ratio $L_{s(o)}/L_{s(a)}$. In practice, it can be expressed by a polynomial function for the shorter segments, because the influence of changes in the shape of the segments is then less marked.

Assumption of a linear dependence of the film thickness ($\alpha = 1$ in Eq. (*1*)) on the linear velocity u or total flow rate Q_t, according to the work of Nord, yields a quadratic relationship between the relative lengthening of the segments and u or Q_t. However, all the experimental evidence in the present work points to power relationships with $\alpha < 1$. The film thickness d_f attains a limiting value at higher flow rates Q_t or linear velocities u as a result of the polynomial dependences of the film thickness d_f on these two parameters (see Fig. 5). Substitution of the values $\eta = 5{\cdot}8 \cdot 10^{-4}$ Pa s and $\gamma_{o/a} = 32{\cdot}8$ mN m^{-1} for chloroform yields the following values

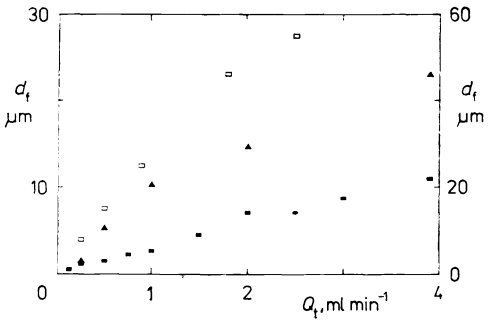

FIG. 5

Experimental relationship between the film thickness and the phase flow rate (ml min^{-1}) for pentanol/water (□ right-hand ordinate, data from ref.[7]) and chloroform/water (L_s = 50 and 15 mm, $L_{s(o)}/L_{s(a)}$ = 2 and 5, ■ and ▲, respectively, left-hand ordinate)

for constant α: 0·39 ± 0·03, 0·45 ± 0·05 and 0·79 ± 0·05, depending on the segment length (values ranging from 0·34 to 0·5 have been found for shorter or longer water segments in air-segmented continuous flow analysis, SCFA (refs[17,18])). This value is probably inversely proportional to the segment length as the "Poiseuille" force increases with the length of the tube distortion.

These conclusions are a result of erroneous interpretation of the experimental dependence between the film thickness (in μm) and the linear velocity u (in cm s^{-1}) for the pentanol/water and chloroform/water systems, given in Fig. 5 of ref.[7]. Recalculating and replotting of Nord's original data[7] gave a strictly nonlinear dependence (Fig. 5, open squares) with values of constants k and α equal to 0·53 ± 0·03 and 0·61 ± 0·05, respectively.

The experimentally determined film thicknesses are lower than those predicted theoretically on the basis of Eq. (*1*) with $k = \alpha = 0{\cdot}67$ or $k = \alpha = 0{\cdot}5$ (ref.[17,18]), as a result of partial destruction of the film by alternating segments of the other, immiscible solvent. The values of the film thickness are higher than those found experimentally for chloroform by Nord[7], as he neglected the effect of the shapes of the leading and tailing ends of the segments on the mean film thickness (he found values that were 3 to 6 times thinner than the calculated values of $d_f = 7$ and 14 μm for $u = 11$ and 23 cm min^{-1} and $d_f = 14{\cdot}6$ μm for $u = 3{\cdot}5$ cm min^{-1}, refs[7,8]).

Film formation also affects the baseline value, as can be seen from the segment shapes at various flow rates of the aqueous phase at constant organic phase flow rate. The length of the aqueous segments increases with increasing total flow rate Q_t and the film is destroyed at a certain defined ratio of the aqueous and organic segment lengths. Above this value, the baseline is identical with that for a stream of water alone. The role of film formation becomes very important at very high flow rates and when the aqueous and organic segments alternate with very high frequency. The film thickness is great and the baseline rapidly increases with increasing flow rate. At very high organic flow rates with short water segments, the baseline signal cannot be compensated and the segment length cannot be measured.

The author wishes to thank Professor Folke Ingman for providing the facilities of the department and for discussions related to the manuscript. He also wishes to thank Assistant Professor Lars-Göran Danielsson for introduction to the field of continuous flow extractions and for a great many stimulating discussions during this work. The financial support from the Swedish National Board for Technical Development and the Swedish Institute is gratefully acknowledged.

LIST OF SYMBOLS

d_f	film thickness
u	linear velocity
Q_o, Q_a, Q_t	flow rates of the organic and aqueous phases, total flow rate ($Q_o + Q_a$)
k, k_u, k_q	constants in Eqs (*1*)–(*4*)
α	constant in Eqs (*1*)–(*4*)

r_o, r_s	radius of the tube (inner) and segment (outer)
η, $\gamma_{o/a}$	viscosity of the organic solvent, surface tension
V_s	volume of sample or segment
L_o, L_s	segment length
S, s_o, S_0	analytical signal, standard deviation of the baseline S_0 value, mean baseline signal
L_{EC}	distance between the injector and detector (length of the "extraction coil")
s_r	relative standard deviation (%)

Subscripts

a	aqueous phase
o	organic phase

REFERENCES

1. Růžička J., Hansen E. H.: *Flow Injection Analysis*, p. 186. Wiley, New York 1988.
2. Valcárel M., Luque de Castro M. D.: *Flow Injection Analysis, Principles and Applications* p. 317. Wiley, New York 1987.
3. Valcárel M., Luque de Castro M. D.: J. Chromatogr. *393*, 3 (1987).
4. Karlsberg B.: Anal. Chim. Acta *214*, 29 (1988).
5. Imasska T., Harada T., Ishibashi N.: Anal. Chim. Acta *129*, 196 (1981).
6. Rossi T. M., Shelly D. C., Warner I. M.: Anal. Chem. *54*, 2056 (1982).
7. Nord L., Karlberg B.: Anal. Chim. Acta *164*, 233 (1984).
8. Lucy C. A., Cantwell F. F.: Anal. Chem. *61*, 107 (1989).
9. Nord L., Bäckström K., Danielsson L. G., Ingman F., Karlberg B.: Anal. Chim. Acta *194*, 221 (1987).
10. Lucy C. A., Cantwell F. F.: Anal. Chem. *61*, 101 (1989).
11. Dasgupta P. K., Lei W.: Anal. Chim. Acta *226*, 255 (1989).
12. Goldsmith H. L., Mason S. G.: J. Colloid. Sci. *18*, 237 (1963).
13. Fossey L., Cantwell F. F.: Anal. Chem. *54*, 1693 (1982).
14. Sweileh J. A., Cantwell F. F.: Can. J. Chem. *63*, 2559 (1985).
15. Bäckström K., Danielsson L. G., Nord L.: Anal. Chim. Acta *187*, 255 (1986).
16. Kubáň V., Danielsson L. G., Ingman F.: Anal. Chem. *62*, 2026 (1990).
17. Snyder L. R., Adler H.: Anal. Chem. *48*, 1017 (1976).
18. Snyder L. R., Adler H.: Anal. Chem. *48*, 1022 (1976).
19. Thommen C., Fromageat A., Obergfell P., Widmer H. M.: Anal. Chim. Acta *234*, 141 (1990).
20. Petersen K., Dasgupta P. K.: Talanta *36*, 49 (1989).

Translation revised by M. Štulíková.